

# Small-Angle X-ray Scattering of Semidilute Rodlike DNA Solutions: Polyelectrolyte Behavior

Lixiao Wang and Victor A. Bloomfield\*

Department of Biochemistry, University of Minnesota, St. Paul, Minnesota 55108

Received February 19, 1991; Revised Manuscript Received May 13, 1991

**ABSTRACT:** Semidilute solutions of persistence length, mononucleosomal DNA ( $160 \pm 5$  base pairs,  $M_r = 1.06 \times 10^6$ ) with and without added salt have been studied by small-angle X-ray scattering (SAXS). The DNA concentration ranged from 30 to 182 mg/mL. The scattering intensity of salt-free solutions displays a broad maximum at scattering vector  $q_m$ , indicative of solution structure caused by the electrostatic and excluded-volume interactions between charged DNA fragments. The peak vanishes when enough salt is added that the screened coulomb potential becomes shorter range than the interparticle distance.  $q_m$  scales with the DNA concentrations as  $C^{1/2}$ . This accords with scaling theory and similar predictions and agrees with SAXS and small-angle neutron scattering results obtained by others on semidilute solutions of semiflexible synthetic polyelectrolytes. When account is taken of the expanded effective DNA diameter in no-salt or low-salt solutions, these solutions have number densities  $\rho$  above the limit  $(\pi d_{\text{eff}} L^2/4)\rho > 4.48$  predicted by Onsager to lead to a transition to an anisotropic, liquid crystalline phase. The peak spacing under these conditions is consistent with hexagonally aligned arrays. However, we observe no evidence of anisotropy. This may be confirmation of the suggestion by Stroobants et al. (1986) that twisting forces between charged rods (for which the crossed orientation has a lower energy than the parallel) raise the concentration required for the transition.

## Introduction

Extensive experimental and theoretical studies have been carried out on the structure of semiflexible synthetic and biological polyelectrolyte solutions using neutron, X-ray, and light scattering techniques. This solution structure depends on several factors, such as the polymer concentration  $C$ , the concentration  $C_s$  of added salt, and the charge density of the polymer chain. A result of the scattering experiments, common to all ionized solutions, is a broad peak, which is sometimes called the Coulomb peak. This peak, with a maximum at scattering vector  $q_m$ , disappears when enough salt is added. In semidilute solutions,  $q_m$  somewhat surprisingly varies with  $C^{1/2}$ , rather than  $C^{1/3}$  as expected from the average intermolecular distance and observed in dilute solutions. These results are summarized in two review articles.<sup>1,2</sup> Similar phenomena have been observed very recently for stiff or rodlike macromolecule solutions.<sup>3</sup>

No definite interpretation of the scattering peak has yet been given in terms of intermolecular solution structure.<sup>1</sup> The proposal of long-range attractive forces advanced by Sogami and Ise<sup>4</sup> has been shown by Overbeek<sup>5</sup> to be invalid. The scaling theory, as introduced by de Gennes et al.<sup>6</sup> and further developed by Odijk,<sup>7</sup> has been useful for understanding some aspects of semidilute polyelectrolyte solutions. The observed dependence of  $q_m$  on  $C^{1/2}$  is in good agreement with the scaling prediction.<sup>1,6,8,11-13</sup> Various theoretical calculations of scattering profiles of polyelectrolyte solutions have been carried out recently.<sup>8,14-18</sup> Monte Carlo simulations of charged rods in aqueous solutions show a liquidlike structure although the maximum of the structure factor is not very pronounced.<sup>14</sup>

A persistence-length double-helical DNA fragment is a highly charged, fairly rigid macromolecule and therefore is suitable for studying the electrostatic interaction between highly charged cylindrical particles in aqueous solutions. Several dynamic and total intensity light scattering studies of mononucleosomal DNA fragments (150–160 base pairs) in dilute solution have been performed as a function of polymer and salt concentration.<sup>19-21</sup> Those studies identified some intriguing dynamic behavior, such

as a transition to a state with an extraordinarily low translational diffusion coefficient. However, they were not able to detect any unusual solution structure associated with such behavior. In the present article we have used small-angle X-ray scattering to probe intermolecular interactions of persistence-length DNA fragments at a scale shorter than accessible to visible light scattering. This length scale, a few hundred angstroms or less, is characteristic of the average intermolecular distance in semidilute solutions and also of the thickness of the Debye-Hückel ion atmosphere in low-salt solutions. It is therefore the appropriate scale to look for solution structure underlying the peculiar dynamics of strongly interacting polyelectrolyte solutions.

Since DNA scatters X-rays rather weakly, fairly high concentrations are needed. The solutions with which we work definitely fall in the semidilute range, for which the number concentration  $\rho$  (molecules/cm<sup>3</sup>) exceeds the inverse of the molecular second virial coefficient for a rod,  $B_2 = (\pi/4)L^2d$ , where  $L$  and  $d$  are the DNA length and diameter. In fact, when increase of the effective diameter in low salt is taken into account,<sup>22</sup> the solution concentrations generally fall above the limit  $B_2\rho = 4.48$ , for which Onsager theory<sup>23</sup> predicts formation of an anisotropic phase. Liquid crystals have been observed at somewhat higher DNA concentrations by SAXS and other techniques.<sup>24,25</sup> That we do not see evidence of liquid crystalline diffraction under our conditions may provide evidence for the theory of Stroobants et al.<sup>26</sup> that twisting forces between polyelectrolytes impede the ordering of charged, rodlike polymers.

## Experimental Methods

**DNA Preparation.** Mononucleosomal DNA was isolated from calf thymus glands as described by Wang et al.<sup>27</sup> Gel electrophoresis and light scattering showed that the molecules contained  $160 \pm 5$  base pairs (bp). This corresponds to a molecular weight of 106 000 and a length of 544 Å. Salt-free DNA was prepared by dialyzing a concentrated preparation against distilled water at 5 °C. Determination of DNA in concentrated solution was made gravimetrically, assuming a density of 1.7 g/mL. Concentrations of more dilute solutions were determined by UV absorbance.

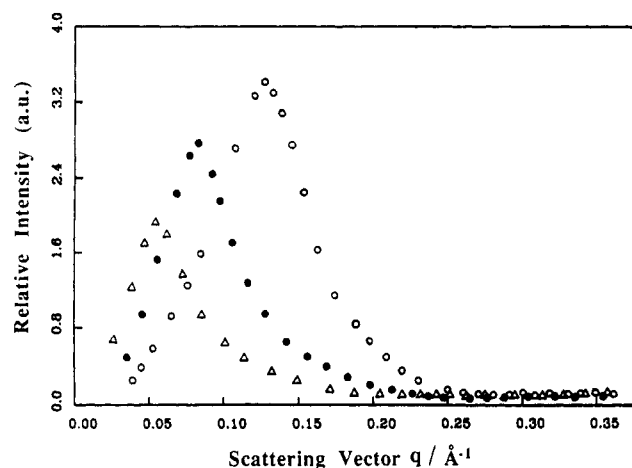


**Figure 1.** DNA concentration dependence of SAXS intensity curves for 160 bp DNA solutions without added salt. DNA concentrations are 182 (○), 72 (●), 30 mg/mL (Δ).

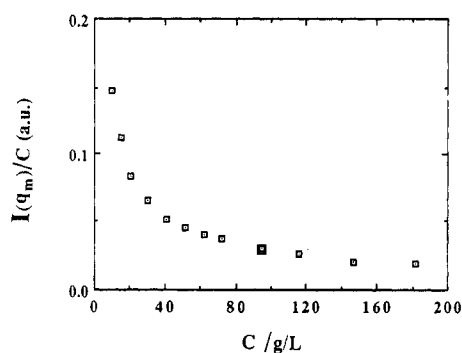


**Figure 2.** DNA concentration dependence of the ratio of the normalized peak intensity.

**SAXS Measurements.** The X-ray source was a rotating-anode generator (RU-200B, Rigaku) operated at 40 kV and 80 mA, producing Cu K $\alpha$ , 1.54-Å radiation. Small-angle X-ray scattering patterns were obtained by using a Kratky camera with a position-sensitive detector (MBRAUN PSD system).<sup>28</sup> Approximately 0.2 mL of the DNA solution was slowly drawn into a syringe through a needle and then injected into a 0.1-mm-diameter glass capillary tube. The sample was maintained at 20 °C, and the camera was evacuated to 20–25 mTorr to reduce the background scattering. The X-ray patterns were usually obtained in 3 h with less than a 1% counting error for the smallest angles. The scattering from a solvent capillary was subtracted from the data after correction for absorption and detector sensitivity. Only relative scattering intensities were obtained; these are reported as a function of the magnitude of the scattering vector  $q = 4\pi \sin \theta / \lambda$ , where  $2\theta$  is the angle between the incident and scattered radiation and  $\lambda$  is the X-ray wavelength. Scattering data were analyzed with computer programs developed by Bohlen<sup>29</sup> at the University of Minnesota. Vonk's method<sup>30</sup> was used to desmear the scattering profiles.

## Results and Discussion

**DNA Concentration Dependence.** Typical scattering curves for rodlike DNA at various concentrations are shown as a function of the scattering vector in Figure 1. Over the concentration range from 30 to 182 mg/mL there is a single broad peak. The peak maximum shifts toward higher angle and greater intensity with increasing DNA concentration, as observed for other polyelectrolyte systems, for example.<sup>3,9–13</sup> This means that the correlation length decreases with increasing DNA concentration, as expected.

The concentration dependence of the normalized peak intensity,  $I(q_m)/C$ , is shown for solutions without added salt in Figure 2. It follows that relationship  $I(q_m)/C \sim C^{-0.72}$  rather than  $C^{-0.5}$  as observed in most other systems<sup>1</sup>

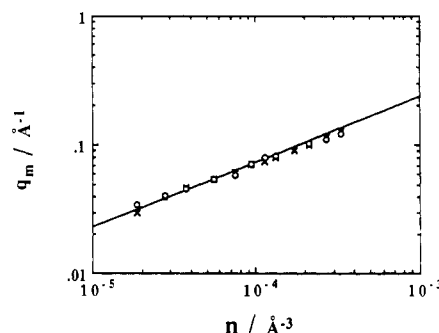


**Figure 3.** Comparison of calculated and experimental values of  $q_m$  for DNA solutions without added salt. The solid curve is calculated from Koyama's equation,  $q_m = 7.24n^{1/2}$  ( $n$  is the number monomer concentration) for semidilute polyelectrolyte solutions without added salt. Two separate series of experiments are identified by (○) and (×).

and predicted by Koyama.<sup>8</sup> We have no ready explanation for this, except to note that intensity measurements involve rather large uncertainties, especially after desmearing. If  $I(q_m)/C$  is divided by the particle scattering factor for rods, the dependence becomes  $C^{-0.27}$ , in equally poor agreement but in the other direction.

Koyama<sup>8</sup> calculated that the maximum scattering vector for semidilute, salt-free polyelectrolyte solutions should be  $q_m = 7.24n^{1/2}$ , where  $n$  is the number concentration of monomer. For dilute solutions without added salt,  $q_m = 3.97(n/N)^{1/3}$  where  $N$  is the degree of polymerization. Figure 3 shows the excellent agreement between our experimental results and the theoretical prediction. Similar agreement has been observed for several synthetic polyelectrolyte systems without added salt.<sup>8,13</sup> These general relations,  $q_m \sim C^{0.5}$  for semidilute solutions and  $q_m \sim C^{1/3}$  for dilute solutions, have been established experimentally and theoretically for several synthetic polyelectrolyte systems.<sup>1,9–13</sup> For rodlike DNA with a length  $L = 3.4 \text{ Å/bp} \times 160 \text{ bp} = 544 \text{ Å}$ , the critical overlap concentration  $C^* \sim 1/L^3 \sim 2 \text{ mg/mL}$ . The concentration range of 10–180 mg/mL examined here is certainly above the critical concentration and is in the semidilute region.

The  $q_m \sim C^{1/3}$  behavior has been observed in SAXS studies of several biopolymer systems, including bovine serum albumin, lysozyme, and tRNA.<sup>31,32</sup> The intermolecular distance obtained by applying Bragg's law to the single broad peak was nearly equal to the intermolecular distance calculated from the polymer concentration by assuming a uniform distribution throughout the solutions. These biopolymers are compact and globular, so the overlap concentrations needed to enter the semidilute regime were not reached.

The full range of behavior for rodlike or stiff polymers is observed by plotting the dimensionless quantity  $q_m L$  vs  $C/C^*$  in Figure 4. The light scattering data for the tobacco mosaic virus ( $L = 3000 \text{ Å}$ , diameter  $d = 180 \text{ Å}$ ) and the fd virus ( $L = 8800 \text{ Å}$ ,  $d = 60 \text{ Å}$ ) are taken from Schulz et al. and Maier et al.<sup>3</sup> The SAXS data for chondroitin sulfate ( $l = 62 \times 6.7 \text{ Å} = 415 \text{ Å}$ ) are taken from Matsuoka et al.<sup>32</sup> The DNA data are from the present work.  $q_m \sim C^{1/3}$  is observed at  $C/C^* < 1$ , and  $q_m \sim C^{1/2}$  at  $C/C^* > 1$ . The transition occurs close to  $C/C^* \approx 1$ . In the case of linear flexible polyelectrolytes,<sup>13</sup> the transition occurred at  $C/C^* \approx 10$ . The difference is presumably due to chain stiffness.

Other theoretical treatments also obtain results in qualitative agreement with experiment. Schneider et al.<sup>14</sup> performed Monte Carlo and perturbation theory calculations for two- and three-bead models of charged, rodlike macromolecules in dilute solution. The position of the

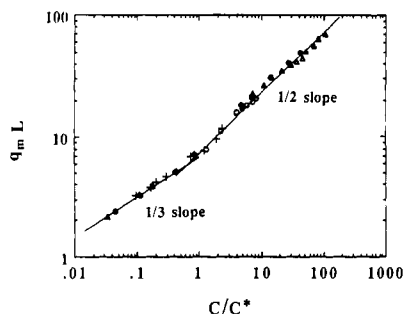


**Figure 4.** Double-logarithmic plot of the position of the SAXS peak maximum in terms of  $q_m L$  vs  $C/C^*$  for several rodlike or stiff polymers. The light scattering data for the tobacco mosaic virus with  $L = 3000$  Å (+,  $\Delta$ ) and fd viruses with  $L = 8800$  Å (O) are taken from Schulz et al.<sup>14</sup> and Maier et al.<sup>14</sup> Data for chondroitin sulfate ( $L = 62 \times 6.7$  Å = 415 Å) (●) are from Matsuoka et al.<sup>32</sup> Our DNA data ( $\Delta$ ) from Figure 3 are also plotted.  $q_m \sim C^{1/3}$  is observed at  $C/C^* < 1$  and  $q_m \sim C^{1/2}$  at  $C/C^* > 1$ . In the overlap regime,  $C/C^* = 1$ , the trends appear to merge.

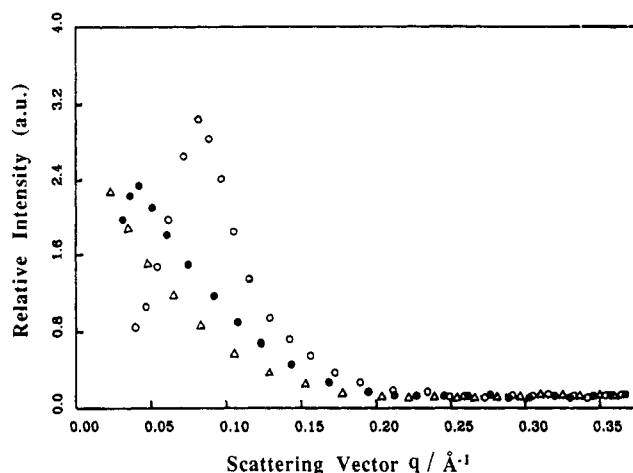


**Figure 5.** NaCl concentration dependence of SAXS intensity curves for 160 bp DNA solutions. DNA concentrations are 70 mg/mL. The NaCl concentrations are 0.001 (●), 0.3 (○), and 0.5 M (Δ).

peak of the angle-averaged radial distribution function was shown to be independent of rod length and thus to depend on concentration as  $C^{1/3}$ . However, the position of  $q_m$  for the full solution structure factor, which is a non-factorizable function of particle and solution contributions, depends on  $L$ . This will cause the concentration dependence of  $q_m$  to approach  $C^{1/2}$  behavior.<sup>14</sup> Benmouna, Genz, and their co-workers<sup>15-17</sup> have used single-component and multicomponent generalizations of the single-contact approximation to calculate scattering from polyelectrolyte solutions. These models are able to reproduce the scattering data qualitatively under many circumstances, though only by large renormalization of the polyelectrolyte charge,  $q_m$  is predicted to vary nearly as  $C^{1/3}$ .

**Salt Concentration Dependence.** SAXS scattering curves of 72 mg/mL solutions of mononucleosomal DNA with various concentrations of added salt are shown in Figure 5.  $q_m$  shifts toward lower scattering vectors with increasing salt concentration (Figure 6), as also observed for several flexible polyelectrolyte systems.<sup>33-35</sup> Initially this shift is slight:  $q_m$  is relatively insensitive to salt concentration until about 0.1 M NaCl, at which value it decreases dramatically. The peak disappears when salt concentration reaches 0.5 M NaCl.

A possible clue to understanding this behavior is to consider the expected peak spacings if the DNA molecules are distributed on average uniformly throughout the

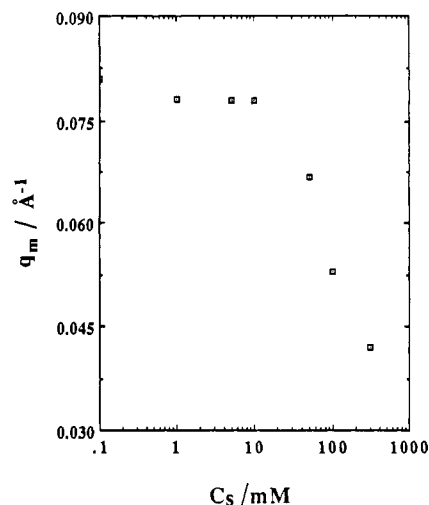


**Figure 6.** Salt concentration dependence of  $q_m$  (peak position at maximum intensity) at a fixed DNA concentration of 72 mg/mL.

solution or are aligned in hexagonal array. Assuming Bragg's law, the calculated peak position is  $q_m = 2\pi/d$ .  $d$ , the average intermolecular distance, is  $d_{\text{uni}} = (M/CN_A)^{1/3}$  for a uniform distribution and  $d_{\text{hex}} = (M_0/N_A C \sin 60^\circ)^{1/2}$  for a hexagonal array.<sup>32</sup> In our solutions,  $C = 0.072$  g/mL,  $l$  (the length per base pair) is  $3.4 \times 10^{-8}$  cm,  $M_0$  (the base-pair molecular weight) is 660, and there are 160 bp/DNA molecule so  $M = 105\,600$ . These values lead to  $q_{m,\text{uni}} = 0.047$  Å<sup>-1</sup> and  $q_{m,\text{hex}} = 0.087$  Å<sup>-1</sup>. The limiting  $q_m$ 's at high and low salt in Figure 6 are reasonably close to these calculated values.

These considerations suggest that there may be a transition from random to parallel arrangement as the salt concentration decreases. This would be in keeping with the suggestion by Onsager<sup>23</sup> that the isotropic-anisotropic transition in a solution of rigid polyelectrolyte rods could be influenced by the increasing diameter of the rod from its hard-cylinder value  $d$  as the ionic strength decreases. Onsager predicted that the solution would be isotropic if the product of second virial coefficient  $B_2$  and number density  $\rho$  is less than 3.34 and anisotropic if  $B_2\rho$  is greater than 4.46. According to Stigter,<sup>22</sup>  $B_2$  is given by

$$B_2 = \pi d_B L^2 / 4 \quad (1)$$

where  $L$  is the rod length and  $d_B$  the effective rod diameter

$$d_B = d + (\ln w + 0.7704) / \kappa \quad (2)$$

where  $\kappa$  is the Debye-Hückel inverse length. Stigter<sup>36</sup> defines the contact potential  $w$  as

$$w = \frac{Z^2 e^2}{DkT\kappa} \frac{2\pi e^{-2x_0}}{\{\beta\gamma x_0 K_1(x_0)\}^2} \quad (3)$$

In this equation,  $Z$  is the charge per unit length along the cylinder axis,  $D$  the dielectric constant,  $x_0$  the rod radius in units of  $\kappa^{-1}$  (i.e.,  $x_0 = \kappa r_0$ , where  $r_0$  is the rod radius), the  $K_1(x_0)$  the modified Bessel function.  $\beta$  and  $\gamma$  are corrections to the Debye-Hückel charge-potential and potential-distance relations, tabulated<sup>36</sup> in terms of  $x_0$  and  $\xi/x_0$  where  $\xi = Ze^2/DkT$ , the ratio of the Bjerrum length  $e^2/DkT$  to the charge spacing  $1/Z$ .

Figure 7 shows plots of  $B_2\rho$  as a function of ionic strength  $I$ , calculated in two different ways. In the first, the ionic strength is just that of the added salt. In the second, which seems more reasonable, the additional contribution from uncondensed Na<sup>+</sup> derived from the DNA is added. According to Manning,<sup>37</sup> if  $\xi > 1$  a fraction  $1 - 1/\xi$  of the

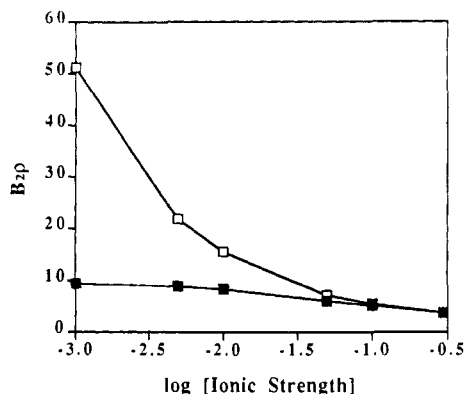


**Figure 7.**  $B_{2\rho}$  as a function of ionic strength for 160 bp DNA at  $C = 72$  mg/mL, calculated according to Stigter<sup>36</sup> with a hard-rod radius  $r_0$  of 12 Å: (□) ionic strength equal to added salt concentration; (■) ionic strength including the additional contribution (0.026 M) from uncondensed  $\text{Na}^+$  derived from the DNA.

polyion charge will be neutralized by condensed or territorially bound counterions. For double-stranded DNA in water, with  $1/Z = 1.7$  Å/charge,  $\xi = 4.18$ . Thus 76% of the DNA charge is neutralized. The remaining 24% of the  $\text{Na}^+$  ions added with the DNA are counted in the solution ionic strength. At a concentration of 72 mg/mL of DNA (0.22 M DNA-P), this is a contribution of 26 mM to the ionic strength. The other values used to compute the curves in Figure 7 from eqs 1–3 are  $L = 544$  Å,  $d = 2r_0 = 24$  Å, and  $\kappa = 3.28 \times 10^7 \text{ l}^{1/2} \text{ cm}^{-1}$ . The number density of DNA molecules is  $4.1 \times 10^{17} \text{ /mL}$ . It is evident from Figure 7 that, at the lowest added salt concentrations,  $B_{2\rho}$  is 1 order of magnitude above the predicted transition regime if only added salt is counted in  $\kappa$ . It is only about 2-fold greater if uncondensed  $\text{Na}^+$  ions are included. In both cases,  $B_{2\rho}$  drops below 4.46 only at the highest added salt concentration, 0.3 M.

Although these results seem to suggest that parallel arrays are forming at the lower salt concentrations, the SAXS profiles (aside from the value of  $q_m$ ) do not support the idea of liquid crystal formation. The peak is broad, there is no evidence of multiple peaks as would be expected for a well-ordered sample, and there was no visual indication of anisotropy (though we did not attempt polarized microscopy). There may, however, be some localized alignment at low salt that permits the formation of microscopic hexagonal domains, leading to the tighter intermolecular spacing and larger  $q_m$ .

The results of Strzelecka and Rill<sup>38</sup> are relevant to our interpretation. They used polarized light microscopy and solid-state  $^{31}\text{P}$  NMR to delineate phase changes in solutions of mononucleosomal DNA at low salt. Their DNA concentrations ranged from 100 to 290 mg/mL. The first indication of a weakly birefringent "precholesteric" phase occurred at about 160 mg/mL, just slightly below our highest concentration of 182 mg/mL. Thus it is consistent with Strzelecka and Rill's results that we do not see overt indications of liquid crystal formation under our conditions. They found that the phase transition behavior depended only weakly on added electrolyte, from 10 mM to 0.2 M. They interpreted this, as we have, to indicate that the effective diameter of the DNA is predominantly determined by the uncondensed  $\text{Na}^+$  from the DNA. However, we have found a large effect of added NaCl on  $q_m$  (Figure 6). This is not necessarily inconsistent with the results of Strzelecka and Rill, since our DNA concentrations are somewhat lower (thus added NaCl plays a greater proportionate role) and since the SAXS profiles

may reflect less extensive and more localized ordering than is observable by microscopy or NMR.

Strzelecka and Rill<sup>38</sup> have also considered the applicability of the theory of Stroobants et al.,<sup>26</sup> finding that, even when the twist associated with electrostatic repulsion between parallel charged cylinders is taken into account, the predicted transition concentrations are significantly lower than those observed. They note that this theory, and that of Onsager<sup>23</sup> on which it is based, assumes very asymmetric rods, while nucleosomal DNA has a more modest axial ratio. Stroobants et al. also observe that polyion flexibility will raise the transition threshold. One hundred sixty base-pair DNA is about one persistence length long, so it is moderately flexible even though commonly described as "rodlike".

## Conclusions

In summary, we have performed small-angle X-ray scattering measurements on highly charged, monodisperse, persistence-length DNA solutions with and without added salt. As with other synthetic polyelectrolytes, a single, broad peak is observed; the peak disappears at high salt. The scattering vector at the peak position is shifted toward larger values with increasing DNA concentration and toward lower values with increasing salt concentration. The  $C^{1/2}$  dependence agrees well with scaling theory predictions, showing that in the semidilute regime short, stiff DNA molecules behave similarly to longer, more flexible polyions. The peculiar decrease of  $q_m$  with increasing salt concentration has also been observed in a variety of flexible and stiff polyion systems.<sup>32–35</sup> With DNA, as with the stiff-chain chondroitin sulfate,<sup>32</sup> there are indications that there may be some local hexagonal alignment of rodlike molecules. This would not be expected for flexible chains and suggests that all occurrences of apparent attraction between polyelectrolytes in low salt may not have a common origin. However, it is equally clear that overtly liquid crystalline phases are not formed at the relatively low concentrations employed here. This is a confirmation of the insight by Stroobants et al.<sup>26</sup> that electrostatic twisting forces will tend to resist the parallel alignment of charged rods, displacing the Onsager transition to higher concentrations. On balance, it appears as though small, localized domains of partial ordering are most likely responsible for the dependence of apparent particle spacing on salt concentration in semidilute solutions of rodlike polyelectrolytes. It is plausible, though not demonstrated, that such local ordering may be related to the unusual dynamic light scattering behavior in these systems.<sup>19–21</sup>

**Acknowledgment.** This work was supported by NSF Grant DMB 88-16433. We gratefully acknowledge Mengtao He, Linda Sauer, and David S. Bohlen for generously making the SAXS facility of the Center of Interfacial Engineering at the University of Minnesota available to us and for help with data analysis.

## References and Notes

- (1) Jannink, G. *Makromol. Chem., Macromol. Symp.* **1986**, *1*, 67.
- (2) Ise, N. *Angew. Chem., Int. Ed. Engl.* **1986**, *25*, 323.
- (3) Maier, E. E.; Schulz, S. F.; Weber, R. *Macromolecules* **1988**, *21*, 1544. Schulz, S. F.; Maier, E. E.; Weber, R. *J. Chem. Phys.* **1989**, *90*, 7.
- (4) Sogami, I.; Ise, N. *J. Chem. Phys.* **1984**, *81*, 6320.
- (5) Overbeek, J. T. C. *J. Chem. Phys.* **1987**, *87*, 4406.
- (6) de Gennes, P.-G.; Pincus, P.; Velasco, R. M.; Brochard, F. *J. Phys. (Paris)* **1976**, *37*, 1461. Hayter, J.; Jannink, G.; Brochard, F.; de Gennes, P.-G. *J. Phys. Lett. (Paris)* **1980**, *41*, L-45.
- (7) Odijk, T. *Macromolecules* **1979**, *12*, 688.

- (8) Koyama, R. *Macromolecules* **1984**, *17*, 1594; **1986**, *19*, 178.  
(9) Drifford, M.; Dalbiez, J. P. *J. Phys. Chem.* **1984**, *88*, 5368.  
(10) Nierlich, M.; Williams, C. E.; Boué, F.; Cotton, J. P.; Daoud, M.; Farnoux, B.; Jannink, G.; Picot, C.; Moan, M.; Wolff, C.; Rinaudo, M.; de Gennes, P.-G. *J. Phys. (Paris)* **1979**, *40*, 701.  
(11) Nierlich, M.; Boué, Lapp, A.; Oberthür, R. *J. Phys. (Paris)* **1985**, *46*, 649; *Colloid Polym. Sci.* **1985**, *263*, 955.  
(12) Nallet, F.; Jannink, G.; Hayter, R.; Oberthür, R.; Picot, C. *J. Phys. (Paris)* **1983**, *44*, 87.  
(13) Kaji, K.; Urakawa, H.; Kanaya, T.; Kitamaru, R. *J. Phys. (Paris)* **1988**, *49*, 993. Kanaya, T.; Kaji, K.; Kitamaru, R.; Higgins, J. S.; Farago, B. *Macromolecules* **1989**, *22*, 1356.  
(14) Schneider, J.; Hess, W.; Klein, R. *Macromolecules* **1986**, *19*, 1729. Schneider, J.; Karrer, D.; Dhont, J. K. G.; Klein R. *J. Chem. Phys.* **1987**, *87*, 3008.  
(15) Benmouna, M.; Weill, G.; Benoit, H.; Akcasu, Z. *J. Phys. (Paris)* **1982**, *43*, 1679.  
(16) Genz, U.; Klein, R.; Benmouna, M. *J. Phys. (Paris)* **1989**, *50*, 449. Genz, U.; Klein, R. *J. Phys. (Paris)* **1989**, *50*, 439.  
(17) Benmouna, M.; Grimson, M. J. *Macromolecules* **1987**, *20*, 1161. Grimson, M. J.; Benmouna, M.; Benoit, H. *J. Chem. Soc., Faraday Trans. 1* **1988**, *84*, 1563.  
(18) Weill, G. *J. Phys. (Paris)* **1988**, *49*, 1049. Martenot, J. P.; Galin, J. C.; Picot, C.; Weill, G. *J. Phys. (Paris)* **1989**, *50*, 493.  
(19) Fulmer, A. W.; Benbasat, J. A.; Bloomfield, V. A. *Biopolymers* **1981**, *20*, 1147.  
(20) Nicolai, T.; Mandel, M. *Macromolecules* **1989**, *22*, 438; **1989**, *22*, 2348.  
(21) Wang, L.; Garner, M. M.; Yu, H. *Macromolecules*, **1991**, *24*, 2368.  
(22) Stigter, D. *Biopolymers* **1977**, *16*, 1435.  
(23) Onsager, L. *Ann. N.Y. Acad. Sci.* **1949**, *51*, 627.  
(24) Luzzati, V.; Nicolaieff, A.; Masson, F. *J. Mol. Biol.* **1961**, *3*, 185.  
(25) Rill, R. L.; Hilliard, P. R., Jr.; Levy, G. C. *J. Biol. Chem.* **1983**, *258*, 250. Strzelecka, T. E.; Rill, R. L. *J. Am. Chem. Soc.* **1987**, *109*, 4513. Strzelecka, T. E.; Davidson, M. W.; Rill, R. L. *Nature* **1988**, *331*, 457.  
(26) Stroobants, A.; Lekkerkerker, H. N. W.; Odijk, T. *Macromolecules* **1986**, *19*, 2232.  
(27) Wang, L.; Ferrari, M.; Bloomfield, V. A. *BioTechniques* **1990**, *9*, 24.  
(28) Kaler, E. W.; Bennett, K. E.; Davis, H. T.; Scriven, L. E. *J. Chem. Phys.* **1983**, *79*, 5673.  
(29) Bohlen, D. S. Ph.D. Thesis, University of Minnesota, 1990.  
(30) Vonk, C. G. *J. Appl. Cryst.* **1971**, *4*, 340; **1975**, *8*, 340.  
(31) Patkowski, A.; Gulari, E.; Chu, B. *J. Chem. Phys.* **1980**, *73*, 4178.  
(32) Matsuoka, H.; Ise, H.; Okubo, T.; Kunugi, S.; Tomiyama, H.; Yoshikawa, Y. *J. Chem. Phys.* **1985**, *83*, 378.  
(33) Ise, N.; Okubo, T.; Kunugi, S.; Matsuoka, H.; Yamamoto, K.; Ishii, Y. *J. Chem. Phys.* **1984**, *81*, 3294.  
(34) Ise, N.; Okubo, T.; Kunugi, S.; Yamamoto, K.; Matsuoka, H.; Kawai, H.; Hashimoto, T.; Fujimura, M. *J. Chem. Phys.* **1983**, *78*, 541.  
(35) Ise, N.; Okubo, T.; Yamamoto, K.; Kawai, H.; Hashimoto, T.; Fujimura, M.; Hiragi, Y. *J. Am. Chem. Soc.* **1980**, *102*, 7901.  
(36) Stigter, D. *Macromolecules* **1982**, *15*, 635.  
(37) Manning, G. S. *Q. Rev. Biophys.* **1978**, *11*, 179.  
(38) Strzelecka, T. E.; Rill, R. L. *Biopolymers* **1990**, *30*, 57.